LETTERS

NMDA receptors are expressed in developing oligodendrocyte processes and mediate injury

Michael G. Salter[1] & Robert Fern[1]

Injury to oligodendrocyte processes, the structures responsible for myelination, is implicated in many forms of brain disorder[1–4]. Here we show NMDA (*N*-methyl-D-aspartate) receptor subunit expression on oligodendrocyte processes, and the presence of NMDA receptor subunit messenger RNA in isolated white matter. NR1, NR2A, NR2B, NR2C, NR2D and NR3A subunits showed clustered expression in cell processes, but NR3B was absent. During modelled ischaemia, NMDA receptor activation resulted in rapid Ca^{2+}-dependent detachment and disintegration of oligodendroglial processes in the white matter of mice expressing green fluorescent protein (GFP) specifically in oligodendrocytes (CNP-GFP mice). This effect occurred at mouse ages corresponding to both the initiation and the conclusion of myelination. NR1 subunits were found mainly in oligodendrocyte processes, whereas AMPA (α-amino-3-hydroxy-5-methyl-4-isoxazole propionic acid)/kainate receptor subunits were mainly found in the somata. Consistent with this observation, injury to the somata was prevented by blocking AMPA/kainate receptors, and preventing injury to oligodendroglial processes required the blocking of NMDA receptors. The presence of NMDA receptors in oligodendrocyte processes explains why previous studies that have focused on the somata have not detected a role for NMDA receptors in oligodendrocyte injury. These NMDA receptors bestow a high sensitivity to acute injury and represent an important new target for drug development in a variety of brain disorders.

Oligodendrocyte injury is central to the loss of function experienced in conditions ranging from cerebral palsy to spinal cord injury and multiple sclerosis[1–4]. Damage to oligodendrocytes is also an important secondary factor in neurological disorders such as stroke[3] and Alzheimer's disease[5]. Oligodendrocytes are responsible for myelinating axons, and loss of myelination under such conditions contributes to brain dysfunction. Myelination is carried out by oligodendrocyte cell processes, and damage to these processes precedes damage to the somata in a number of disease models (for example, see refs 1, 2, 6, 7). This may indicate a heightened sensitivity to injury in these structures. In human diseases, 'dying back' of oligodendrocyte processes may be seen (for example, in multiple sclerosis[8,9]), suggesting that this is a clinically relevant phenomenon.

Oligodendrocytes express Ca^{2+}-permeable glutamate receptors and have low resistance to oxidative stress, two factors that make them particularly susceptible to injury[3,6,10–12]. They are thought to express mainly non-NMDA glutamate receptors, and this expression is developmentally regulated[13,14]. The high expression of non-NMDA receptors in immature oligodendrocytes and low expression of the calcium-impermeable GluR2 subunit at the point when they initiate myelination may increase their sensitivity to an excitotoxic cascade mediated by ischaemic glutamate release and subsequent intracellular Ca^{2+} ($[Ca^{2+}]_i$) overload[3,13,14]. This may explain the selective injury of precursor oligodendrocytes and subsequent hypomyelination in periventricular leukomalacia (PVL). PVL is the main injury associated with cerebral palsy, the most common human birth disorder. The long-term consequences of PVL can involve either focal oligodendrocyte loss (associated with early loss of cell processes

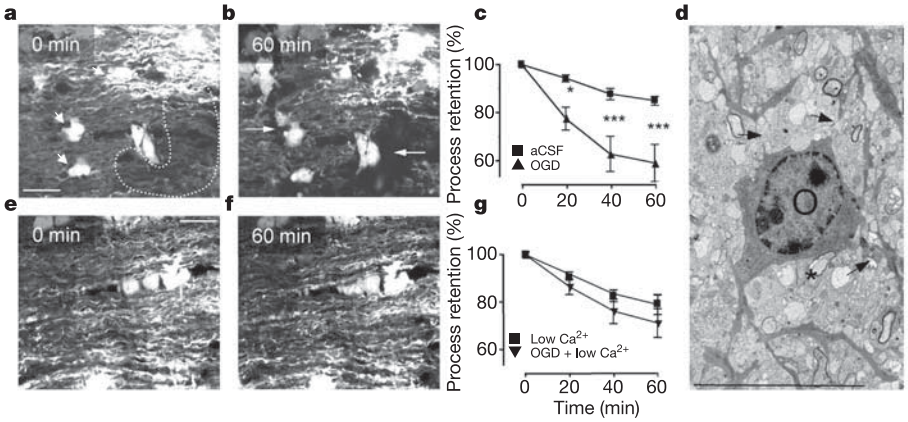

Figure 1 | Ischaemia results in rapid loss of oligodendroglial process. **a**, **b**, CNP-GFP oligodendrocytes before (0 min) and after 60 min OGD. Processes are lost over time (arrowheads show oligodendroglial somata, arrows show areas denuded of processes). **c**, Process retention during perfusion with artificial cerebrospinal fluid (aCSF) (squares) or during OGD (triangles). Statistical significance is shown for OGD versus aCSF (*, $P \leq 0.005$; ***, $P \leq 0.001$), determined by ANOVA. Error bars show s.e.m. **d**, Oligodendrocyte (labelled 'O') ultrastructure after 60 min OGD. Arrows indicate detached processes, asterisk shows a myelinated axon. **e**, **f**, Control perfusion at 0 min and 60 min. **g**, Process retention, showing no significant difference between OGD and OGD under conditions of low Ca^{2+} ($P > 0.01$). Scale bars, 10 μm.

[1]Department of Cell Physiology and Pharmacology, University of Leicester, Leicester LE1 9HN, UK.

© 2005 Nature Publishing Group

in animal models) or diffuse disruption of myelination, associated with abnormal oligodendrocyte process morphology[1].

Live mouse optic nerve oligodendroglia expressing GFP under the control of the 2′-3′-cyclic nucleotide 3′-phosphodiesterase gene promoter (CNP) were imaged by confocal microscopy at postnatal day 10 (P10). The development of rodent white matter is delayed compared with humans, and this preparation correlates developmentally to the fetal white matter susceptible to PVL[15,16]. The morphology of the oligodendrocytes conformed to previous descriptions, characterized by primary processes radiating from the somata and numerous myelinating processes running parallel to axons[17]. Process morphology was visible in detail and was generally stable for periods of >60 min during control perfusion (Fig. 1c, e, f). This was assessed both by monitoring mean pixel intensity in large regions of interest drawn around somata-free areas (for example, dashed line in Fig. 1a), and by visual inspection using a graded scoring system (by an observer blind to the experimental conditions; see Methods).

To examine changes in oligodendrocyte morphology, the optic nerves were subjected to oxygen-glucose deprivation (OGD). During OGD, loss of processes occurred rapidly, with significant loss at 20 min and further deterioration at 40 min and 60 min (Fig. 1a–c). After 60 min of OGD, large areas denuded of GFP-stained processes were apparent (arrows in Fig. 1b). As processes deteriorated, they frequently detached from neighbouring regions of the same process and/or the somata while retaining GFP fluorescence, indicating the temporary formation of membrane-delineated structures. Formation of swellings within processes was also common. In line with previous studies, ultrastructural examination of oligodendroglial cells that survived 60 min of OGD revealed a loss of cell processes in many cases[6] (Fig. 1d and Supplementary Fig. 1). Process detachment was confirmed by examination of serial sections. Loss of processes during ischaemia was abolished by lowering extracellular Ca^{2+} to ~30 μM (90 μM EGTA+120 μM Ca^{2+}) (Fig. 1g) (note that low Ca^{2+} reduces fluorescence somewhat). Removing extracellular Ca^{2+} attenuated acute oligodendroglial cell death during OGD[6,11] and had a similar protective effect on oligodendroglial somata in the optic nerve (Fig. 2i).

Using 30 μM NBQX (2,3-dioxo-6-nitro-1,2,3,4-tetrahydrobenzo[f]quinoxaline-7-sulphonamide) to block Ca^{2+} influx through AMPA/kainate receptors during OGD had no effect upon the loss of processes (Fig. 2a, b, e) but prevented the loss of oligodendrocyte somata (Fig. 2i). Therefore, although OGD-induced injury to oligodendrocyte processes is Ca^{2+}-dependent, unlike in the somata the route of Ca^{2+} influx is not AMPA/kainate receptors. The widespread loss of processes resulting from OGD in the presence of NBQX was characterized by detachment of membrane-delineated processes close to the soma and by the presence of large vacuoles within processes (Fig. 2g). The presence of vacuoles in these degenerating processes might correspond to the bright GFP puncta that form during OGD, and might represent the loci where processes are detaching to form temporary membrane-delineated fragments.

The unexpected injury to processes in the presence of NBQX led us to investigate alternative potential sources of Ca^{2+} influx. When the selective NMDA receptor blocker MK801 (10 μM) was co-applied with NBQX, injury to processes was largely prevented (Fig. 2c–e) and oligodendroglia retained numerous fine processes attached to the somata (Fig. 2h). Significant protection was also achieved by MK801

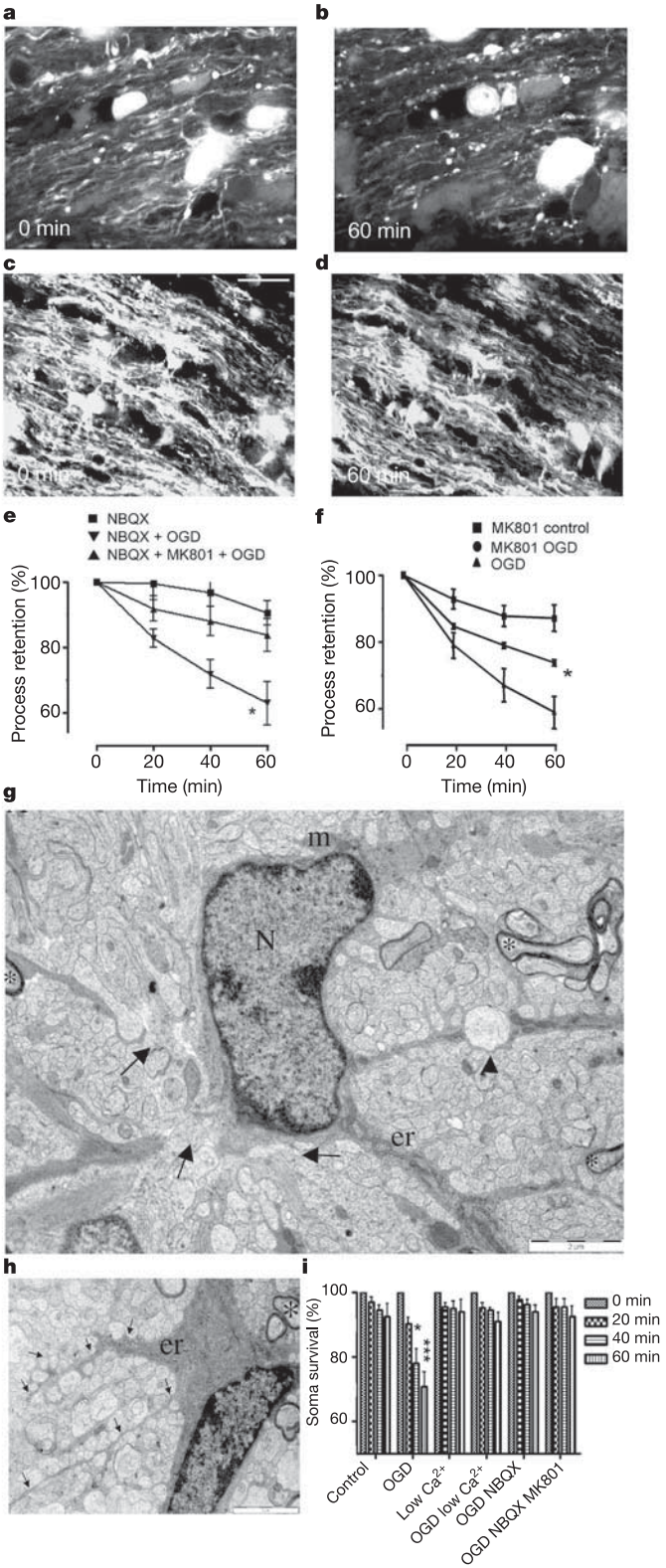

Figure 2 | NMDA receptor activation destroys oligodendrocyte processes. **a**, **b**, Perfusion with NBQX before and after 60 min ODG. **c**, **d**, NBQX+MK801 before and after 60 min OGD. **e**, Process retention during treatment with NBQX (significance tested by ANOVA versus control aCSF), NBQX+OGD (tested versus OGD alone) or NBQX+MK801+OGD (tested versus NBQX+OGD). **f**, Perfusion with MK801 under normoxic conditions had no significant effect. MK801 in the absence of NBQX was significantly protective against process loss during OGD (tested versus OGD). Error bars in **e**, **f** indicate s.e.m.; *, $P \leq 0.005$. **g**, Oligodendrocyte exposed to OGD for 60 min in the presence of NBQX. Arrows indicate detached processes. N, nucleus; m, mitochondria; er, endoplasmic reticulum; asterisk, myelinating axon. **h**, Oligodendrocyte exposed to NBQX+MK801+OGD for 60 min. Note the intact processes radiating from the soma (arrows). **i**, Oligodendroglial soma death at four time points (0, 20, 40, 60 min) under various conditions. Error bars indicate s.e.m.; significance tested versus control; *, $P \leq 0.005$; ***, $P \leq 0.001$. Scale bars, 10 μm (**a**–**d**), 2 μm (**g**, **h**).

© 2005 Nature Publishing Group

in the absence of NBQX, but MK801 had no effect when applied under normoxic conditions (Fig. 2f). Although ifenprodil (10 μM), an NMDA antagonist with selectivity for the NR2B subunit, was mildly protective at $t = 20$ min when applied with NBQX (Supplementary Fig. 2a; $P < 0.05$), it did not protect at 60 min. Perfusion with 1 mM NMDA (+10 μM glycine, no Mg^{2+}) under normoxic conditions did not result in significant damage to oligodendrocyte processes (Supplementary Fig. 2b), presumably reflecting the capacity of the processes to buffer Ca^{2+} influx when an adequate energy supply is available.

The above data suggest differential expression of ionotropic glutamate receptors on oligodendrocytes, with AMPA/kainate receptors expressed on somata and NMDA receptors on processes. GFP fluorescence was retained in optic nerves fixed with paraformaldahyde, and clustered expression of the NMDA receptor subunit NR1 was detected along oligodendroglial processes, using antibodies against two different regions of the NR1 subunit (Fig. 3a and Supplementary Fig. 3a). Blinded counting (by a naive observer) of NR1 clusters yielded a 57.1 ± 4.4% (mean ± s.e.m.) overlap with GFP ($n = 6$ sections). NR1 subunit expression was absent from astrocytes, as examined in P10 mice expressing GFP under the control of the GFAP promoter[18] (Supplementary Fig. 4b). NR1 clusters were seen in 27.8 ± 4.4% of neurofilament-200-positive axons in wild-type FVB/N mice ($n = 4$ sections; Supplementary Fig. 4a). The occasional presence of NR1 clusters in neurofilament-200-positive axons is expected, given the close apposition of axons and oligodendrocyte processes and the resolving power of confocal imaging.

NR2A, -B, -C, -D and NR3A subunit expression was also seen in oligodendrocytes (Fig. 3b–f) but NR3B staining was absent. Double-labelling for NR1 and NR2A in wild-type optic nerve revealed a high degree of subunit co-localization on processes (Fig. 3b). The non-NMDA glutamate receptor subunit GluR4 was robustly expressed mainly in oligodendroglial somata (Fig. 3g), as were GluR2/3 subunits, but to a lesser extent (Supplementary Fig. 3b). A similar, largely somatic expression of AMPA/kainate receptors, with low or no expression on cell processes, has been noted in immature oligodendrocytes in other *in situ* preparations (for example, ref. 19).

Previous studies have failed to detect *NR1* mRNA in the rat optic nerve[20]. Here we used fluorescence polymerase chain reaction with reverse transcription (RT–PCR), coupled to a high stringency RNA extraction protocol involving three sequential purifications steps (see Methods). We found *NR1* transcript in the optic nerve (Fig. 3h), which when quantified was at 1–2% of the abundance found in the whole brain (Supplementary Fig. 6; see ref. 21). Extraction blanks run alongside samples were negative for both *NR1* and actin, and the *NR1* product was sequenced and found to correlate to the correct portion

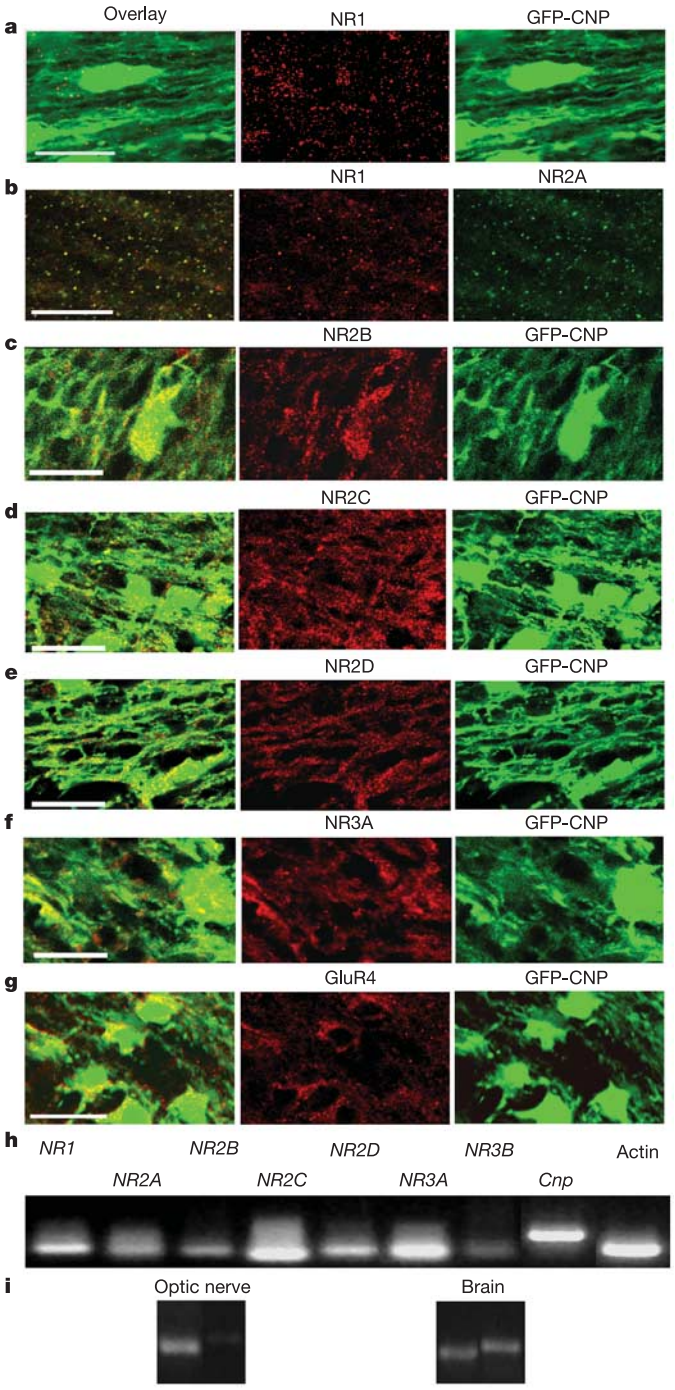

Figure 3 | Oligodendrocytes express NMDA receptors in clusters on cell processes and AMPA/kainate receptors diffusely on somata. **a**, NR1 (red) is expressed in clusters mainly in oligodendroglial (green) processes. **b**, NR1 (red) and NR2A (green) in wild-type optic nerve. **c**–**f**, NR2B (**c**, red), NR2C (**d**, red), NR2D (**e**, red) and NR3A (**f**, red) expression in CNP-GFP optic nerve, showing expression on oligodendrocytes (green). **g**, GluR4 (red) expression in oligodendrocyte somata (green) in CNP-GFP optic nerve. **h**, PCR products in whole optic nerve, showing the presence of *NR1*, *NR2A*, *NR2B*, *NR2C*, *NR2D* and *NR3A* NMDA receptor subunits, and the virtual absence of *NR3B*. **i**, PCR products for intron regions of *NR1* (left lane) and *Thy1* (right lane) in whole brain and optic nerve. The *NR1* intron is present in optic nerve and brain, but the *Thy1* intron is effectively present only in brain. Scale bars, 10 μm. See Supplementary Fig. 5 for control staining.

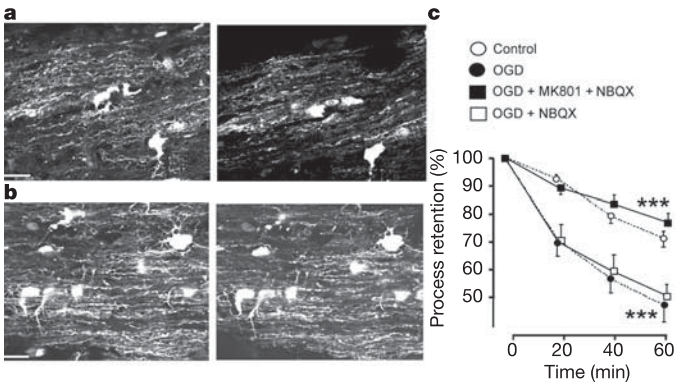

Figure 4 | Ischaemia results in rapid loss of oligodendroglial process in P25 optic nerve. **a**, Process loss in oligodendrocytes during OGD in the presence of NBQX, at 0 min (left) and 60 min (right). **b**, Process loss during OGD in the presence of NBQX+MK801, at 0 min (left) and 60 min (right). Note that in both cases the somata are retained but processes are lost when MK801 is absent. **c**, Process retention during OGD treatment (significance tested by ANOVA versus control), NBQX+OGD (tested versus OGD) or NBQX+MK801+OGD (tested versus NBQX+OGD). ***, $P \leq 0.001$. Error bars indicate s.e.m. Scale bars, 10 μm.

© 2005 Nature Publishing Group

of the *NR1* complementary DNA. PCR quantification revealed 2,000–3,000-fold lower abundance of the neuron-specific marker *Thy1* in the optic nerve compared with the oligodendrocyte-specific marker CNPase (this ratio was approximately 1:1 in whole brain), indicating a corresponding level of certainty that the optic nerve PCR product is glial in origin. The presence of trace *Thy1* mRNA levels within axons is consistent with previous observations showing protein synthesis within axons[22].

To examine the origin of *NR1* and *Thy1* mRNA in the optic nerve, we performed RT–PCR for intron regions of *NR1* and *Thy1*, which exist only in the nucleus. This revealed robust expression of the *NR1* intron in whole brain and optic nerve, whereas expression of the *Thy1* intron was detected in whole brain but not in the optic nerve (Fig. 3i). Optic nerve *Thy1* mRNA is therefore produced in somata that are not present in the nerve (that is, retinal ganglion cells), whereas NR1 is produced in optic nerve glial somata. PCR analysis of all known NMDA receptor subunits revealed the presence of mRNA for the subunits detected by antibody staining in oligodendrocytes (Fig. 3h). Quantification relative to actin levels suggests that *NR1*, *NR2C* and *NR3A* mRNA are the most abundant subunits in whole optic nerve; *NR2B* mRNA was present at low abundance, and *NR3B* was effectively absent.

In addition to cerebral palsy, oligodendrocyte process injury is relevant to adult diseases such as stroke, spinal cord injury and multiple sclerosis[2–4]. We therefore examined process loss in P25 CNP-GFP mouse optic nerve, a stage by which effectively all precursor cells have progressed to the mature oligodendrocyte phenotype[23]. Antibody staining revealed a similar pattern of NR1, NR2A and NR2B expression in oligodendrocytes at this stage, with abundant GluR2/3 expression mainly in somata (Supplementary Fig. 7). GFP fluorescence was relatively stable in these mature oligodendrocytes during control perfusion, but OGD evoked rapid and severe process loss (Fig. 4c). As with the P10 nerve, the loss of processes was not significantly affected by NBQX but was abolished by NBQX+MK801 (Fig. 4a–c).

A companion paper to this one (ref. 24) describes NMDA receptor currents in oligodendrocytes in several brain regions and at various developmental stages. These NMDA receptor-mediated currents show a low degree of voltage-dependent Mg^{2+} block, and immunostaining results indicate that NR1, NR2C and NR3 are the major NMDA receptor subunits, but NR2A and NR2B are also present. Our PCR and immunostaining results show similar patterns of expression of the main subunits, and the presence of robust NR2C and NR3A subunit expression indicates a similar, low Mg^{2+} block. Several reports suggest low Ca^{2+} permeability in NMDA receptors that incorporate the NR1A, NR2A/NR2B and NR3A subunits[25,26]. However, no information is available regarding the Ca^{2+} permeability of receptors that include the NR2C subunit, which may not share this feature when incorporated with NR3A. Furthermore, the dimensions of oligodendrocyte processes are small, and even NMDA receptors with low Ca^{2+} permeability may raise intracellular Ca^{2+} to toxic levels within such a confined space. Our data clearly show the Ca^{2+}-dependence of NMDA receptor-mediated process loss, and indicate that sufficient Ca^{2+} influx occurs through the NMDA receptors on processes to result in injury.

There is evidence for the presence of NMDA receptors on mature astrocytes, Muller cells and Bergman glia[13], and some evidence for their presence on oligodendrocytes in other preparations[27,28]. Activation of the AMPA/kainate receptors expressed by developing oligodendroglia can influence gene transcription and cell proliferation, survival and fate[13]. The functional significance of NMDA receptor expression in immature oligodendroglial processes is unclear and might involve axon–glial signalling during myelinogenesis. Myelin initiation begins with the extension of multiple processes from the somata that make contact with axons[17]. At this point, oligodendroglial processes will either proceed with myelination or retract from the axon. How this decision is controlled is unclear, but Ca^{2+} influx through activated NMDA receptors would affect cytoskeletal elements within the processes and could determine stabilization/retraction. Regardless of the function of NMDA receptors on developing oligodendrocyte processes, their pathophysiological relevance is high, as they confer a sensitivity to injury that is likely to have significance for a variety of neurological diseases. It is encouraging that our results show that NMDA receptor blockade alone can be sufficient to protect against injury. The unusual subunit composition of the receptors (which include mainly NR2C in addition to NR3A subunits) also raises the prospect of developing targeted interventions with fewer side effects than those experienced with non-selective NMDA antagonists.

METHODS

Animals and tissue analysis. Transgenic mice (FVB/N) carrying the enhanced GFP sequence (EGFP) under the control of mouse CNP promoters 1 and 2 (ref. 29) were donated by the laboratory of V. Gallo. Mice were backcrossed to wild-type FVB/N females to the third generation to reduce GFP expression levels. Animals were maintained in accordance with UK Home Office regulations. Optic nerves were dissected at P7–13, sealed in an atmospheric perfusion chamber at 37 °C and imaged using an Olympus IX70 confocal microscope. Optic nerves were perfused and exposed to ischaemic conditions using established protocols (see ref. 6).

Loss of GFP-filled processes was assessed as a change in mean pixel intensity within about three large representative (in terms of process density and brightness), soma-free regions of interest (ROI, see Fig. 1a) per flattened image stack ($200 \times 200 \times 15\,\mu m$ thick). This will underestimate fluorescence changes in processes owing to the incorporation of process-free areas. ROI intensity changes were analysed by analysis of variance (ANOVA), with all experiments within a group compared at each time point (Tukey's post-hoc test). For all figures, one asterisk, $P \leq 0.005$; three asterisks, $P \leq 0.001$. There was no correlation between the initial GFP brightness and the changes seen during OGD or during drug treatments. In addition, image stacks were scored by eye (blind to treatment) for process damage, using the following scoring system: 0, no change apparent; 1, detectable loss of processes; 2, clear loss of processes; 3, severe loss of processes; 4, a few processes retained; 5, only a few GFP puncta retained; 6, complete loss of processes. Scored analyses were tested using Kruskal–Wallis tests with Tukey's post-hoc tests, and in all cases confirmed the changes detected by pixel intensity analysis (data not shown). Imaging parameters and laser settings were unchanged throughout each experiment.

Immunohistochemistry. For immunohistochemistry, optic nerves were dissected in 0.1 M PBS and fixed in 4% paraformaldehyde for 30 min. Optic nerves were then incubated in 0.1 M PBS plus 20% sucrose (w/v) for 5 min before freeze-sectioning and subsequent incubation in 0.1 M PBS, 10% of an appropriate fetal serum, 0.5% Triton X-100 and primary antibody overnight at 4 °C. Separate polyclonal antibodies raised against the NR1 subunit amino terminus (rabbit, Upstate) or carboxy terminus (goat, Santa Cruz) were used at 1:200. Rabbit polyclonal antibodies raised against GluR4 and GluR2/3 (Upstate) were used at 1:200. Goat polyclonal antibodies raised against NR2A, NR2B, NR2C and NR2D (Upstate) were used at between 1:100 and 1:500. Rabbit polyclonal anti-NR3A and anti-NR3B antibodies (Santa Cruz) were used at 1:100. Monoclonal anti-neurofilament-200 (NF-200) antibody (Alomone) was used at 1:100. Appropriate Alexa-conjugated secondary antibodies (Cambridge Bioscience) were used at 1:1,000 and were applied for 2 h after washing.

RT–PCR. Tissue was ground up in liquid nitrogen and subjected to a triazol extraction. RNA was then column-purified (RNeasy lipid RNA mini kit, Qiagen) and the resulting RNA treated to remove DNA contamination (DNAfree, Ambion). The RNA was purified by extraction with phenol (Sigma) pH 4.2, and resuspended to a concentration of $1\,\mu g\,\mu l^{-1}$. RT–PCR was performed on 1–3 μg of the RNA samples using Omniscript (Qiagen) according to the manufacturer's instructions (all quantities were doubled). The reverse-transcribed mix (2 μl) was then used for fluorescence PCR in the SYBR green system using Quantitect SYBR green PCR master mix (Qiagen) with a 40 μl reaction volume. See Supplementary Fig. 8 for primer sequences. All primers were tested on whole brain as a positive control. Primers were optimized for >90% efficiency (95 °C for 45 s, 57 °C for 30 s, 72 °C for 45 s, for 40 cycles with a dissociation curve at the end).

Electron microscopy. Optic nerves were subjected to 60 min of OGD before washing in Sorenson's buffer and fixation in 3% glutaraldehyde/Sorenson's. Nerves were post-fixed with 2% osmium tetroxide and dehydrated before infiltration in epoxy. Sections were counterstained with uranyl acetate and lead citrate, and examined using a Jeol 100CX electron microscope. Electron

© 2005 Nature Publishing Group

micrographs were collected by R.F., who was blind to the experimental procedure used to produce each sample.

Received 27 July; accepted 10 October 2005.

1. Back, S. A. *et al.* Selective vulnerability of late oligodendrocyte progenitors to hypoxia-ischemia. *J. Neurosci.* **22,** 455–463 (2002).
2. Grossman, S. D., Rosenberg, L. J. & Wrathall, J. R. Temporal–spatial pattern of acute neuronal and glial loss after spinal cord contusion. *Exp. Neurol.* **168,** 273–282 (2001).
3. Dewar, D., Underhill, S. M. & Goldberg, M. P. Oligodendrocytes and ischemic brain injury. *J. Cereb. Blood Flow Metab.* **23,** 263–274 (2003).
4. Pitt, D., Werner, P. & Raine, C. S. Glutamate excitotoxicity in a model of multiple sclerosis. *Nature Med.* **6,** 67–70 (2000).
5. Brun, A. & Englund, E. A white matter disorder in dementia of the Alzheimer type: a pathoanatomical study. *Ann. Neurol.* **19,** 253–262 (1986).
6. Wilke, S., Salter, M., Thomas, R., Allcock, N. & Fern, R. Mechanism of acute ischemic injury of oligodendroglia in early myelinating white matter: the importance of astrocyte injury and glutamate release. *J. Neuropathol. Exp. Neurol.* **63,** 872–881 (2004).
7. Ludwin, S. K. Pathology of demyelination and remyelination. *Adv. Neurol.* **31,** 123–168 (1981).
8. Rodriguez, M., Scheithauer, B. W., Forbes, G. & Kelly, P. J. Oligodendrocyte injury is an early event in lesions of multiple sclerosis. *Mayo Clin. Proc.* **68,** 627–636 (1993).
9. Wolswijk, G. Oligodendrocyte survival, loss and birth in lesions of chronic-stage multiple sclerosis. *Brain* **123,** 105–115 (2000).
10. Back, S. A., Gan, X., Li, Y., Rosenberg, P. A. & Volpe, J. J. Maturation-dependent vulnerability of oligodendrocytes to oxidative stress-induced death caused by glutathione depletion. *J. Neurosci.* **18,** 6241–6253 (1998).
11. Fern, R. & Moller, T. Rapid ischemic cell death in immature oligodendrocytes: a fatal glutamate release feedback loop. *J. Neurosci.* **20,** 34–42 (2000).
12. Follett, P. L., Rosenberg, P. A., Volpe, J. J. & Jensen, F. E. NBQX attenuates excitotoxic injury in developing white matter. *J. Neurosci.* **20,** 9235–9241 (2000).
13. Gallo, V. & Ghiani, C. A. Glutamate receptors in glia: new cells, new inputs and new functions. *Trends Pharmacol. Sci.* **21,** 252–258 (2000).
14. Itoh, T. *et al.* AMPA glutamate receptor-mediated calcium signalling is transiently enhanced during development of oligodendrocytes. *J. Neurochem.* **81,** 390–402 (2002).
15. Small, R. K., Riddle, P. & Noble, M. Evidence for migration of oligodendrocyte–type-2 astrocyte progenitor cells into the developing rat optic nerve. *Nature* **328,** 155–157 (1987).
16. Craig, A. *et al.* Quantitative analysis of perinatal rodent oligodendrocyte lineage progression and its correlation with human. *Exp. Neurol.* **181,** 231–240 (2003).
17. Butt, A. M. & Ransom, B. R. Morphology of astrocytes and oligodendrocytes during development in the intact rat optic nerve. *J. Comp. Neurol.* **338,** 141–158 (1993).
18. Zhuo, L. *et al.* Live astrocytes visualized by green fluorescent protein in transgenic mice. *Dev. Biol.* **187,** 36–42 (1997).
19. McDonald, J. W., Althomsons, S. P., Hyrc, K. L., Choi, D. W. & Goldberg, M. P. Oligodendrocytes from forebrain are highly vulnerable to AMPA/kainate receptor-mediated excitotoxicity. *Nature Med.* **4,** 291–297 (1998).
20. Matute, C., Sanchez-Gomez, M. V., Martinez-Millan, L. & Miledi, R. Glutamate receptor-mediated toxicity in optic nerve oligodendrocytes. *Proc. Natl Acad. Sci. USA* **94,** 8830–8835 (1997).
21. Salter, M. G., Franklin, K. A. & Whitelam, G. C. Gating of the rapid shade-avoidance response by the circadian clock in plants. *Nature* **426,** 680–683 (2003).
22. Alvarez, J., Giuditta, A. & Koenig, E. Protein synthesis in axons and terminals: significance for maintenance, plasticity and regulation of phenotype. With a critique of slow transport theory. *Prog. Neurobiol.* **62,** 1–62 (2000).
23. Barres, B. A. *et al.* Cell death and control of cell survival in the oligodendrocyte lineage. *Cell* **70,** 31–46 (1992).
24. Káradóttir, R., Cavelier, P., Bergersen, L. H. & Attwell, D. NMDA receptors are expressed in oligodendrocytes and activated in ischaemia. *Nature* doi:10.1038/nature04302 (this issue).
25. Matsuda, K., Kamiya, Y., Matsuda, S. & Yuzaki, M. Cloning and characterization of a novel NMDA receptor subunit NR3B: a dominant subunit that reduces calcium permeability. *Brain Res. Mol. Brain Res.* **100,** 43–52 (2002).
26. Sasaki, Y. F. *et al.* Characterization and comparison of the NR3A subunit of the NMDA receptor in recombinant systems and primary cortical neurons. *J. Neurophysiol.* **87,** 2052–2063 (2002).
27. Wang, C. *et al.* Functional *N*-methyl-D-aspartate receptors in O-2A glial precursor cells: a critical role in regulating polysialic acid–neural cell adhesion molecule expression and cell migration. *J. Cell Biol.* **135,** 1565–1581 (1996).
28. Ziak, D., Chvatal, A. & Sykova, E. Glutamate-, kainate- and NMDA-evoked membrane currents in identified glial cells in rat spinal cord slice. *Physiol. Res.* **47,** 365–375 (1998).
29. Yuan, X. *et al.* Expression of the green fluorescent protein in the oligodendrocyte lineage: a transgenic mouse for developmental and physiological studies. *J. Neurosci. Res.* **70,** 529–545 (2002).

Supplementary Information is linked to the online version of the paper at www.nature.com/nature.

Acknowledgements We wish to thank V. Gallo for the gift of CNP-GFP mice, I. Eperon for discussion, J. Alix for immunostaining advice, and N. Alcock for technical assistance with electron microscopy. This work was supported by a grant from the National Institutes of Neurological Disorders and Stroke to R.F.

Author Information Reprints and permissions information is available at npg.nature.com/reprintsandpermissions. The authors declare no competing financial interests. Correspondence and requests for materials should be addressed to R.F. (rf34@le.ac.uk).

© 2005 Nature Publishing Group